

AMC and HARQ: How to Increase the Throughput

Mohammed Jabi, Leszek Szczecinski, Mustapha Benjillali, Abdellatif Benyoussef, and Benoit Pelletier

Abstract—In this work, we consider transmissions over block fading channels and assume that adaptive modulation and coding (AMC) and hybrid automatic repeat request (HARQ) are implemented. Knowing that in high signal-to-noise ratio, the conventional combination of HARQ with AMC is counterproductive from the throughput point of view, we adopt the so-called layer-coded HARQ (L-HARQ). L-HARQ allows consecutive packets to share the channel and preserves a great degree of separation between AMC and HARQ; this makes the encoding and decoding very simple and allows us to use the available/optimized codes. Numerical examples shown in the paper indicate that L-HARQ can provide significant throughput gains compared to the conventional HARQ. The L-HARQ is also implemented using turbo codes indicating that the throughput gains also materialize in practice.

Index Terms—AMC, Block Fading Channels, Channel Coding, HARQ, Hybrid Automatic Repeat reQuest, Incremental Redundancy, Rate Adaptation.

I. INTRODUCTION

IN this work, we are interested in increasing the throughput of the physical layer (PHY) when the coded information is transmitted using equal-length channel blocks which are subject to independent fading. We are motivated by two main results. First, by [1], which demonstrates that using the conventional hybrid ARQ (HARQ) when adaptive modulation and coding (AMC) is adopted decreases the throughput at high signal-to-noise ratio (SNR). The second result is due to [2], [3] which proposes layer-coded HARQ (L-HARQ) – a simple encoding/decoding scheme tailored to improve the throughput of HARQ. However, L-HARQ was studied when the instantaneous channel state information (CSI) was not available at the transmitter; i.e., without the AMC. In this work we propose to leverage the knowledge of instantaneous CSI and incorporate it in the coding scheme of L-HARQ.

A. Background

AMC is adopted for communications over time-varying channels to guarantee an efficient use of channel resources. It relies on a feedback channel over which the receiver informs the transmitter about the “best” transmission rate to use. This rate is evaluated by the receiver based on the estimated CSI.

M. Jabi was with INRS, Montreal, Canada; he is now with Nokia Poland. [e-mail: jabi.mohamed@gmail.com].

L. Szczecinski, and A. Benyoussef are with INRS, Montreal, Canada. [e-mail: leszek@emt.inrs.ca, benyoussef@emt.inrs.ca].

M. Benjillali is with the Communication Systems Department, INPT, Rabat, Morocco. [e-mail: benjillali@ieee.org].

Benoit Pelletier is with InterDigital Canada, Ltée., Montreal, Canada. [e-mail: Benoit.Pelletier@interdigital.com]

Despite this rate adaptation, transmission errors are unavoidable in practice, and they are handled by the retransmission protocol, HARQ.

HARQ also uses feedback channel: one-bit messages inform the transmitter about the decoding success (positive acknowledgment (ACK)) or failure (negative acknowledgment (NACK)). After each NACK, the transmitter starts a new HARQ *round* (i.e., a retransmission) which conveys additional information necessary to decode the packet; in other words, HARQ encodes the packet *across* the transmission rounds. The HARQ *cycle*, defined as the sequence of transmission rounds of the same packet, terminates if the packet is correctly received (as indicated by ACK). If the number of rounds is limited, HARQ is said to be *truncated*; then, the NACK in the final round indicates a *packet loss*.

Both, AMC and HARQ may be considered as parts of PHY, and their interaction has been addressed vastly in the literature. For instance, [4]–[9] analyzed the throughput, while [10]–[13] focused on the delay due to HARQ. In all these works, a constraint on the probability of packet loss was imposed; by doing so, the value of HARQ was highlighted as, indeed, HARQ efficiently decreases the probability of having packets lost at the end of the cycle. This is different from our work because we ignore the packet loss and only sheer throughput is considered; the rationale for such an approach is discussed in Sec. II-E.

To meaningfully compare different AMC/HARQ strategies, it is important to assume that the resources used by the PHY are fixed.¹ This goal can be attained by encoding one packet over the whole channel block in each round; such HARQ is said to be *conventional*, and was often used as a basis for theoretical analysis, e.g., [17].

However, as demonstrated in [1], this conventional approach can actually be detrimental to the throughput; that is, AMC alone is better than AMC combined with the conventional HARQ. This surprising, at first sight, result is caused by the fact that the conventional HARQ is not fully adaptive: it uses the CSI only in the first transmission round [18] of a given packet; reusing next the entire channel block for each round

¹First, this is because the block fading model implicitly assumes that the duration of all transmissions is the same. More importantly, from a methodological point of view, the transmission with variable PHY resources is more relevant in the context of multi-user communications, which also implies some form of resource management; then, drawing useful conclusions may be difficult analyzing solely the PHY. Thus, fixing the resources of the point-to-point PHY, we are able to isolate HARQ from the external factors; such as a multi-user scheduling [14], [15] or a cooperative transmission [16]; which may be combined with HARQ but are difficult to characterize.

causes a waste of resources.²

Indeed, the literature already recognizes that, to improve the throughput, the coding across the HARQ rounds must be modified. The most relevant solutions may be classified as *i)* a *multi-packet coding* [2], [3], [20], [21], where many packets with variable contents are jointly encoded into fixed-length codewords which then use the fixed resources (channel blocks) or, as *ii)* a *variable-length coding* [22]–[27], where rather the codewords length varies throughout the HARQ rounds and the packet content is fixed.³

We focus this work on the adaptive multi-packet coding whose advantage over the relatively well-studied variable-length coding will be discussed in Sec. III-A.

B. Contribution and Organization

The main difficulties of the multi packet coding are *i)* the practicality of joint encoding/decoding of many packets, and *ii)* the rate adaptation of this joint coding. This was already apparent in the case of multi-packet coding when the instantaneous CSI was not available at the transmitter [21, Sec. V].

To make the multi-packet approach practical, we will use L-HARQ, studied in [2], [3] and implemented via a two-step (or, layered) approach, where the joint coding is implemented in two independent steps: the binary packet mixing is followed by the conventional channel coding. From the theoretical perspective, when compared to a more general joint coding/decoding scheme [21], [30], L-HARQ does not impose any throughput penalty [30, Th. 3]. It is also more practical as it can be used with commercially available encoders/decoders [3]. The remaining issue is how to use L-HARQ with AMC, that is, how to exploit the CSI in all transmission rounds and yet maintain the simple layered-coding strategy.

The main contribution of this work lies, therefore, in the generalization of L-HARQ [2], [3] to take advantage of the CSI in all rounds of HARQ. The proposed encoding scheme yields a fully adaptive HARQ: like in [2], [3], the CSI observed in the previous rounds of the same packet is exploited but, unlike [2], [3], each round exploits as well the instantaneous (possibly outdated) CSI.

The question which needs to be answered in this context is: how to adjust the coding rates using the rich information about the CSI? We formulate the optimization problem and propose a framework to solve it. Concluding on the excessive numerical complexity of the latter, we present heuristic rate-adaptation policies inspired by the optimal adaptation policy used in the AMC and by the results of [3]. The proposed solution leads to a local adaptation with easily adjustable parameters and does not require the knowledge of the entire model of the relationship between the different HARQ rounds, the AMC, and the fading model.

²We will comment on this in Example 2, but note here that a somehow similar behavior of the throughput is also observed in HARQ transmissions without CSI: for high SNR, the throughput of HARQ improves only negligibly [19], [20] when the number of rounds increases.

³We also note that similar ideas are discussed in [28], where the *fixed-to-variable* (here, *variable-length*) and *variable-to-fixed* (here, *multi-packet*) coding strategies are defined. In fact, the Long Term Evolution (LTE) standard enables the variable-length coding [29, Ch. 12.1] varying the number of the so-called resource blocks [29, Ch. 9.1] on a per HARQ-round basis.

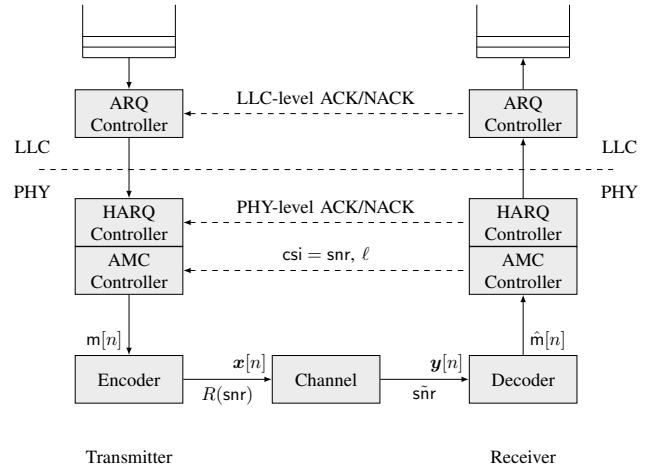


Fig. 1. Model of the transmission of the packet $m[n]$: AMC chooses the rate based on the CSI, csi , provided by the receiver before the transmission begins; here, the CSI is the same as the SNR and with a finite number of rates, it is enough to transmit the index of the rate, ℓ , and the transmission rate is then given by $R(\text{snr}) = R_{[\ell]}$. The LLC layer implements the ARQ which ensures the error-free transmission and makes the throughput of the PHY the unique criterion for comparison, see Sec. II-E.

To the best of our knowledge, the literature does not provide such a solution to adapt *simultaneously* the AMC and HARQ, while keeping the channel resources fixed. The most practical element is that the adaptation we propose relies on the error-rate curves of the commercial encoders/decoders that can be easily acquired. This is critical from the implementability perspective. In fact, rare are works which include the practical encoders/decoders, mainly because the decoding error-rate curves after many HARQ rounds are difficult to obtain and to use; for example, a significant part of [24] (which implements a variable-length HARQ) is dedicated to the issue of approximating these curves and the results are limited to three HARQ rounds.

The rest of the paper is organized as follows. In Sec. II we introduce the adopted models while the principle of the proposed L-HARQ is explained in Sec. III. The optimization issues are discussed in Sec. III-D and Sec. III-E. Sec. IV compares the proposed L-HARQ to the alternative strategies using examples of *i)* the idealized encoders/decoders, and *ii)* the practical turbo-codes. The conclusions are drawn in Sec. V.

II. MODEL

A. AMC

In a point-to-point transmission over a block fading channel, illustrated in Fig. 1, we assume that the size, N_s , of the transmission blocks, $x[n]$, does not change with their index n ; the transmitter encodes the packet $m[n] \in \{0, 1\}^{RN_s}$ into a codeword $x[n] = \Phi[m[n]] \in \mathcal{X}^{N_s}$, where $\Phi[\cdot]$ is the encoder, R – the coding rate, and \mathcal{X} – the constellation set of size $M = |\mathcal{X}|$.

We assume that the choice of the rate is done at the receiver using the estimated CSI, csi , that is, $R = R(csi) \in \mathcal{R}$, where \mathcal{R} is the set of available rates. To simplify the examples, let

will consider frequency non-selective channel, where the CSI is uniquely represented by the SNR, snr .

While, for theoretical considerations we may sometimes assume a continuous-valued set $\mathcal{R} = \mathbb{R}_+$ is available, in practice, the set of available rates is discrete, i.e., $\mathcal{R} = \{R_{[1]}, \dots, R_{[L]}\}$ and then it is enough to transmit the *index* $\ell \in \{1, \dots, L\}$ of the chosen rate, that is $R(\text{snr}) = R_{[\ell]}$; here, L denotes the number of available rates.

In all examples, \mathcal{X} will be a M -ary quadrature amplitude modulation (QAM) constellation (with $M = 4$ or $M = 16$); the empirical error-rate curves of the practical encoders/decoders will be obtained using the turbo encoding/decoding. We emphasize that, independently from how the coded modulation is implemented, there is always a maximum rate which cannot be exceeded; in our case, this limitation is expressed as $R_{[L]} < \log_2(M)$.

Assuming that packets are always available at the transmitter (the buffer is saturated), the codeword $\mathbf{x}[n]$ is transmitted in the n th block, and the receiver observes the signal

$$\mathbf{y}[n] = \sqrt{\text{s}\tilde{\text{n}}r[n]} \mathbf{x}[n] + \mathbf{z}[n], \quad (1)$$

where $\mathbf{z}[n]$ is a vector of realizations of zero mean, unit-variance, complex Gaussian variables, modeling the noise. Since $\mathbf{x}[n]$ are (realizations of) random variables uniformly distributed over \mathcal{X} , with appropriate normalization of the latter, $\text{s}\tilde{\text{n}}r[n]$ is the SNR at the receiver experienced at the time the transmission is carried out.

In general, $\text{s}\tilde{\text{n}}r \neq \text{snr}$, and this SNR ‘‘mismatch’’ is caused by the estimation errors and/or by the delay between the time the SNR, $\text{snr}[n]$, is estimated and the time the transmission is carried out with the experienced SNR, $\text{s}\tilde{\text{n}}r[n]$.⁴

The receiver tries to decode the transmitted packet $\mathbf{m}[n]$ using the channel outcome

$$\hat{\mathbf{m}}[n] = \text{DEC}[\mathbf{y}[n]]. \quad (2)$$

The decoding errors $\text{ERR}[n] = \{\hat{\mathbf{m}}[n] \neq \mathbf{m}[n]\}$ that occur due to different, simultaneously occurring events (such as e.g., atypical noise, interference, or fading) are characterized by a packet error rate (PER) function

$$\text{PER}(\text{snr}; R) \triangleq \Pr \{ \text{ERR} | \text{SNR} = \text{snr}, R \}, \quad (3)$$

which, for a given R , decreases monotonically with snr . This function captures the behavior of the entire receiver from the point of view of the transmitter and includes the effect of the decoding, channel estimation, and synchronization. It also captures the effect of delayed/imperfect CSI as follows

$$\text{PER}(\text{snr}; R) = \mathbb{E}_{\text{S}\tilde{\text{N}}R} \left[\text{PER}^{\text{rx}}(\text{S}\tilde{\text{N}}R; R) | \text{SNR} = \text{snr} \right] \quad (4)$$

where

$$\text{PER}^{\text{rx}}(\text{s}\tilde{\text{n}}r; R) \triangleq \Pr \left\{ \text{ERR} | \text{S}\tilde{\text{N}}R = \text{s}\tilde{\text{n}}r, R \right\}, \quad (5)$$

⁴Although the time index of both SNRs refers to the same n th channel block, the estimation must be carried out before the transmission takes place; it has to be done sufficiently early to leave a time for a feedback of the index ℓ and to allow the transmitter to encode/modulate the packet. Thus, there is always a delay between the moments of estimation and transmission.

is the PER function of the receiver and depends on the SNR, $\text{s}\tilde{\text{n}}r$, actually observed and experienced during the transmission.

In practice, it is not necessary to estimate/measure the entire PER function and it is sufficient to find the SNR interval limits $\gamma_{[\ell]}$ which satisfy a constraint on PER when transmitting with rate $R_{[\ell]}$ [1, Sec. III], i.e.,

$$\gamma_{[\ell]} = \min_{\text{snr} \in \mathbb{R}^+} \{ \text{snr} : \text{PER}(\text{snr}; R_{[\ell]}) \leq \epsilon \}, \quad (6)$$

where $\epsilon \in \mathbb{R}^+$ denotes a PER constraint. This approach can be related to the calibration of the LTE receivers which, observing the CSI (here the SNR, snr), should report the largest rate $R_{[\ell]} \in \mathcal{R}$ for which the inequality condition in (6) is satisfied with $\epsilon = 10^{-1}$ [31, Sec. 7.2]. That is, the calibration process in LTE implicitly solves (6). The coding adaptation for HARQ we will propose, exploits the PER curves (or the SNR intervals) and thus preserves the legacy and adaptation simplicity of current systems.

B. Channel Model

We will model $\text{snr}[n]$ as realizations of independent, identically distributed (i.i.d.) random variables $\text{SNR}[n]$, which is appropriate if the transmission of the channel blocks $\mathbf{x}[n]$ is well separated in time.⁵

The derivations will be done in abstraction of a particular fading type, but in the numerical examples, we assume Rayleigh fading, i.e., $\text{SNR}[n]$ is drawn from an exponential distribution

$$p_{\text{SNR}}(\text{snr}) = 1/\overline{\text{snr}} \exp(-\text{snr}/\overline{\text{snr}}), \quad (7)$$

where $\overline{\text{snr}}$ is the average SNR, and we have removed the time-indexing $[n]$ that is irrelevant with the i.i.d. modeling of the SNRs.

The variables $\text{SNR}[n]$ and $\text{S}\tilde{\text{N}}R[n]$ are, in general, mutually dependent. Again, for the sake of numerical examples, we assume that the SNR experienced during the transmission, $\text{S}\tilde{\text{N}}R$, is a delayed version of the SNR estimated at the receiver, SNR ,⁶ and their joint probability density function (PDF) is given by [32], [33]

$$p_{\text{SNR}, \text{S}\tilde{\text{N}}R}(\text{snr}, \text{s}\tilde{\text{n}}r) = \frac{1}{(1-\delta)\overline{\text{snr}}} I_0 \left(\frac{2\sqrt{\delta\text{snr}\text{s}\tilde{\text{n}}r}}{(1-\delta)\overline{\text{snr}}} \right) \cdot \exp \left(-\frac{\text{s}\tilde{\text{n}}r + \text{snr}}{(1-\delta)\overline{\text{snr}}} \right), \quad (8)$$

where I_0 is the zero-order modified Bessel function of the first kind, and δ is the correlation factor

$$\delta = J_0^2(2\pi f_D \tau). \quad (9)$$

⁵In the LTE, the channel blocks are attributed to many users in a time-interleaved manner. So, here, the blocks $\mathbf{x}[n]$ correspond to a particular user but are attributed in non-adjacent time instants. This time-separation allows to account for the round-trip delay due to the propagation, and the processing at the receiver and the transmitter.

⁶As we said before, snr is estimated first by the receiver, used by the transmitter to adapt the rate $R(\text{snr})$, and the transmission is finally carried out with the SNR $\text{s}\tilde{\text{n}}r$.

Here, τ is the time difference between the instants of estimation and transmission, f_D is the Doppler frequency, and J_0 is the zero-order Bessel function of the first kind. Essentially the same relationship will be obtained if we assume that the difference between $\tilde{\text{snr}}$ and snr is due to channel estimation errors [34, eq. (20)].

Example 1 (Threshold decoding). *Assume that the receiver's PER function is binary*

$$\text{PER}^{\text{rx}}(\tilde{\text{snr}}; R_{[\ell]}) = \mathbb{I}[\tilde{\text{SNR}} < \gamma_{[\ell]}^{\text{th}}], \quad (10)$$

where the indicator function $\mathbb{I}[a] = 1$ if a is true, and $\mathbb{I}[a] = 0$ otherwise; and $\gamma_{[\ell]}^{\text{th}}$ is uniquely defined by the transmission rate $R_{[\ell]}$.

If the joint distribution of SNR and $\tilde{\text{SNR}}$ is defined by (8), the PER function (3) is calculated using (4) as

$$\text{PER}(\text{snr}; R_{[\ell]}) = \Pr \left\{ \tilde{\text{SNR}} < \gamma_{[\ell]}^{\text{th}} \mid \text{SNR} = \text{snr}, R_{[\ell]} \right\} \quad (11)$$

$$= Q_1 \left(\sqrt{\frac{2\delta \text{snr}}{(1-\delta)\tilde{\text{snr}}}}, \sqrt{\frac{2\gamma_{[\ell]}^{\text{th}}}{(1-\delta)\tilde{\text{snr}}} \right), \quad (12)$$

where we used the form of the (complementary) cumulative density function (CDF) of a non-central chi-square distribution [35, Sec. 2.3] with $Q_m(\cdot, \cdot)$ being the generalized Marcum Q -function.

C. Throughput-Optimal Rate Adaptation

The throughput is defined as the long-term average number of successfully received bits per transmitted symbol, or channel use, (bit/cu) and, since we use constant-length blocks, we can write it as

$$\eta = \lim_{N \rightarrow \infty} \frac{1}{N} \sum_{n=1}^N R[n], \quad (13)$$

where $R[n]$ denotes the number of decoded bits normalized by the block length, N_s , i.e., $R[n] \in \{0, R(\text{snr}[n])\}$. It is also called a *reward* in the n -th block.

The mean reward (expectation taken with respect to the decoding error events, ERR) is given by $R(1 - \text{PER}(\text{snr}; R))$ and, since we model $\text{snr}[n]$ by i.i.d. random variables, the time-average from (13) may be replaced by the expectation [1], [34]

$$\eta^{\text{amc}} = \mathbb{E}_{\text{SNR}} \left[R(\text{SNR}) \cdot \left(1 - \text{PER}(\text{SNR}; R(\text{SNR})) \right) \right]. \quad (14)$$

To find the rate adaptation function $R(\text{snr})$ which maximizes η^{amc} , we can enter with the maximization under the expectation operator in (14) and the throughput-optimal rate adaptation function $R(\text{snr})$ of the AMC is then found by solving the following one-dimensional optimization problem (for each value of snr)

$$R(\text{snr}) = \underset{R \in \mathcal{R}}{\text{argmax}} R(1 - \text{PER}(\text{snr}; R)). \quad (15)$$

In practice, $R(\text{snr})$ is monotonically increasing with snr , which is in line with our intuition: for high SNR (or, more generally, for high-quality CSI), a larger transmission rate is used and a larger throughput is obtained.

So, for the discrete rates we identify the *decision regions* of the SNR, $[\gamma_{[\ell]}, \gamma_{[\ell+1]})$ such that the rate adaptation is defined as

$$R_{[\ell]} = R(\text{snr}) \iff \text{snr} \in [\gamma_{[\ell]}, \gamma_{[\ell+1]}), \quad (16)$$

where $\gamma_{[1]} \triangleq 0$, $\gamma_{[L+1]} \triangleq \infty$.

We mention briefly that the solutions of (15) and (6) do not, in general, produce the same decision regions. The choice of the one or the other criterion to define the SNR limits $\gamma_{[\ell]}$ is an implementation issue.

We emphasize here that, while the throughput (14) depends on the distribution $p_{\text{SNR}}(\text{snr})$, the optimal adaptation function, $R(\text{snr})$ – does not. In fact, the distribution $p_{\text{SNR}}(\text{snr})$ is most likely not known in practice, so using the rate-adaptation (15) or (16) which are oblivious to the knowledge of $p_{\text{SNR}}(\text{snr})$ is a desirable feature. Of course, the PER function $\text{PER}(\text{snr}; R_{[\ell]})$ may depend on the probabilistic model of the relationship between SNR and $\tilde{\text{SNR}}$ as we saw in Example 1; however, such a relationship will still be captured by $\gamma_{[\ell]}$, see (6); these SNR interval limits are then optimal irrespectively of the marginal distribution $p_{\text{SNR}}(\text{snr})$ required to calculate the expectation in (14).

Fine-tuning the adaptation

The rate adaptation defined by (15) is throughput-optimal, however, we may use $R(\text{snr})$ with additional heuristics targeting the error rates. Namely, we can artificially change the argument of the rate-adaptation function $R(\cdot)$ in (16) and use the rate

$$R \leftarrow R(\text{snr}\Delta); \quad (17)$$

for $\Delta < 1$, it provides a more “conservative” adaptation: the same rates $R_{[\ell]}$ will be used in higher SNRs (comparing to $\Delta = 1$), which leads to a smaller probability of decoding error. On the other hand, the rate-adaptation is more “aggressive” with $\Delta > 1$ which allows the transmitter to use higher rates at the cost of larger probability of error. This simple modification of the adaptation strategy which relies on a fine-tuning of one parameter, Δ , will be exploited later.

Performance limit

Since we do not consider power adaptation in this work, the throughput is always upper-bounded by the ergodic capacity of the channel [17], [32], [36]

$$\eta \leq \bar{C} \quad (18)$$

$$\bar{C} \triangleq \mathbb{E}_{\text{SNR}}[I(\text{SNR})], \quad (19)$$

where $I(\text{snr}) = I(X; Y | \text{snr})$ is the mutual information (MI) between the random variables $X \in \mathcal{X}$ and Y modeling respectively the channel input and output.

The limit (19) can be attained in the idealized case when *i)* SNR = $\tilde{\text{SNR}}$, *ii)* capacity achieving codes are used, *iii)* the transmission rate set \mathcal{R} is continuous, and *iv)* the rates are adapted as $R(\text{snr}) = I(\text{snr})$ [32]; then, the receiver's PER function (5) is binary, i.e., $\text{PER}^{\text{rx}}(\tilde{\text{snr}}; R) = \mathbb{I}[I(\tilde{\text{snr}}) < R]$; this is similar to the assumption we made in Example 1 with $\gamma_{[\ell]}^{\text{th}} = I^{-1}(R_{[\ell]})$.

D. HARQ

If retransmissions are allowed, the packet $m \in \{0, 1\}^{R_{[\ell]} \cdot N_s}$ is encoded into K subcodewords, $\mathbf{x}_k = \Phi_k[m] \in \mathcal{X}^{N_s}$, where $\Phi_k[\cdot], k = 1, \dots, K$, are the encoding functions, and K is the maximum number of transmissions for each packet. We consider here incremental redundancy HARQ (IR-HARQ), that is, all the subcodewords \mathbf{x}_k are complementary (punctured) versions of a mother codeword, $\mathbf{x}_0 = [\mathbf{x}_1, \dots, \mathbf{x}_K]$.

Then, each round carries a different subcodeword \mathbf{x}_k , and the transmission outcome of the k -th round is given by

$$\mathbf{y}_k = \sqrt{\tilde{\text{snr}}_k} \mathbf{x}_k + \mathbf{z}_k, \quad k = 1, \dots, K, \quad (20)$$

where we eliminate the time-index n from (1) and rather use the ‘‘packet-centric’’ notation, indexing the HARQ rounds with k ; thus, $\tilde{\text{snr}}_k$ is the SNR at the receiver in the k -th HARQ round. The important point in the ‘‘conventional’’ IR-HARQ is that the rate is chosen in the first round, i.e., $R_{[\ell]} = R^{\text{harq}}(\text{snr}_1)$.

The question which should be answered now is: how to find the HARQ throughput-optimal rate adaptation $R^{\text{harq}}(\text{snr}_1)$?

Since HARQ introduces memory, the optimal rate-adaptation function $R^{\text{harq}}(\text{snr})$ depends on the distribution of the SNR and is quite difficult to find.⁷ This clashes with the simplicity of the AMC rate-adaptation (15) which does not depend on the distribution $p_{\text{SNR}}(\text{snr})$, see comments after (16).

Fine-tuning strategy (17) might be used as a practical alternative. However, optimizing/fine-tuning $R^{\text{harq}}(\text{snr}_1)$ is not always worth the effort: we know from [1, Prop. 4] that, using HARQ on top of the AMC, actually penalizes the throughput if we consider the region of high SNR. This happens, independently of how we choose the rate adaptation function $R^{\text{harq}}(\text{snr}_1)$, because HARQ adapts the rate to the CSI only in the first round and it ignores the CSI observed in the subsequent rounds [1, Sec. V.D].

To remedy this problem and make HARQ aware of the CSI in each round, various approaches have been proposed in the literature. One simple strategy suggested in [1] relies on the AMC rate-adaptation function, i.e., $R^{\text{harq}}(\text{snr}) = R(\text{snr})$ and applies the so-called *packet dropping*, which in some cases terminates the HARQ cycle before the K -th round is reached and a NACK is received.

This works as follows: in each round, the rate that might be offered by the AMC, $R(\text{snr}_k)$ is compared to the rate chosen in the first round, $R(\text{snr}_1)$. Rather than insisting on retransmitting the packet with a low nominal rate $R(\text{snr}_1)$, PHY is allowed to take advantage of the observed SNR by transmitting a new packet with a high-rate $R(\text{snr}_k)$. The packet is then dropped before the k -th round starts (and, instead, a first round of a new packet begins) [1, Sec. VI.A]

$$R(\text{snr}_k) > R(\text{snr}_1) \implies \text{Drop the packet.} \quad (21)$$

The packet-dropping is also ‘‘backward compatible’’ in the sense that it uses the same signaling as the conventional IR-HARQ and occupies the same bandwidth. It eliminates the

throughput penalty imposed by the IR-HARQ but does not improve the throughput significantly.

A natural question that arises is how the packet dropping *combines* with a better rate-adaptation strategy $R^{\text{harq}}(\text{snr})$. Again, we would like to avoid the formal dependence on the channel model so we may use the simplified tuneable adaptation defined in (17) with $\Delta > 1$. Indeed, by being more aggressive, we are exposed to a higher probability of undecoded packet, but we will mitigate this effect by leveraging the very principle of retransmissions proper to HARQ.

Example 2 (16-QAM, Rayleigh fading, threshold decoding). *To show an example of throughput, we have to define how the decoding errors occur in HARQ. To this end, we adopt the simplified threshold-decoding principle we used in Example 1 and assume that the block length, N_s , is sufficiently large so that the error occurs if the average accumulated MI at the receiver is lower than the transmission rate [17], that is,*

$$\text{ERR}_k = \left\{ \sum_{l=1}^k I(\tilde{\text{SNR}}_l) < R(\text{SNR}_1) \right\}. \quad (22)$$

For 16-QAM, the MI function $I(\text{snr})$ can be obtained numerically using the method from [37, Sec. 4.5]. Thus, the values of SNRs in (22) determine the decoding error ERR_k .

We also consider here the idealized case of a continuous rates set, $\mathcal{R} = [0, 4)$. Then, we obtain the AMC-optimal rate adaptation function $R(\text{snr})$ solving (15) with the PER function defined by (12), where i) due to continuity of the rate set \mathcal{R} , we remove the index $[\ell]$ and ii) we replace $\gamma_{[\ell]}^{\text{th}}$ by $I^{-1}(R(\text{snr}))$.⁸

Fig. 2 presents the throughput of the conventional IR-HARQ compared to the ergodic capacity \bar{C} . The results indicate that increasing the number of rounds from 1 to 4 not only does not increase the throughput but, actually, is detrimental. Comparing with the similar results in Fig. 5 this effect is less pronounced if we decrease the correlation between the estimated- and the instantaneous SNRs, i.e., for a larger normalized Doppler frequencies $f_D \tau$.

To explain these results, we can consider two successively observed SNRs, snr_1 and snr_2 , such that $\text{snr}_1 \ll \text{snr}_2 \implies R(\text{snr}_1) \ll R(\text{snr}_2)$. We assume that a new HARQ cycle starts with snr_1 and the first round experiences a decoding failure, i.e., NACK is declared to the transmitter at the end of the first round. Using HARQ, the same packet will be retransmitted with the maximum possible reward $R(\text{snr}_1)$. On the other hand, if only one transmission is allowed, i.e., we use the AMC, the transmission of a new packet starts with a possible reward $R(\text{snr}_2) \gg R(\text{snr}_1)$. Thus, the reward of the AMC is larger than the one attainable by HARQ. It happens because HARQ ignores the CSI in the second transmission; this effect was analyzed in [1] where the penalty of using HARQ in high SNR is formally demonstrated.

This also explains the rationale behind the packet dropping. If $R(\text{snr}_2) > R(\text{snr}_1)$, according to (21) we start the trans-

⁷In particular, because the decision regions are not simply defined by the intervals (16), [1].

⁸We note here that, since we are considering only 16-QAM modulation in this example, ‘‘AMC’’ has a somehow oxymoronic meaning of ‘‘AMC with fixed modulation’’. This is not a critical issue since we are interested in using the PER curves of the receiver, irrespectively how the coding/modulation is implemented.

mission of the new packet (that is, we drop/abandon the old one). The throughput of packet dropping, $\eta_4^{\text{ir,drop}}(\hat{\Delta})$, is also shown in Fig. 2, where $\hat{\Delta} > 1$ is the optimal “aggressiveness” factor, see (17), chosen to maximize the throughput for each value of the average SNR $\overline{\text{snr}}$, i.e., $\hat{\Delta}$ is obtained as follow

$$\hat{\Delta} = \underset{\Delta \in \mathbb{R}^+}{\text{argmax}} \eta(R(\text{snr}\Delta)), \quad (23)$$

where $\eta(R(\text{snr}))$ is the throughput using the rate adaptation policy $R(\text{snr})$. In the numerical examples, $\hat{\Delta}$ is obtained through the exhaustive research above the neutral value $\Delta = 1$.⁹

As stated before, the packet dropping removes the detrimental effect of HARQ but helps little in improving the throughput in its “high” range: for $\eta^{\text{amc}} > 2.5 \text{ bit/cu}$, we observe $\eta^{\text{amc}} \approx \eta_4^{\text{ir,drop}}(\hat{\Delta})$.

We also show the throughput of the conventional HARQ with the aggressive rate adaptation denoted by $\eta_4^{\text{ir}}(\hat{\Delta})$, where no improvement over the conventional HARQ η_4^{ir} is noted. Again, this is merely a confirmation of the formal statement made in [1], which demonstrated that, for high SNR, irrespectively of the rate-adaptation policy, the throughput of HARQ must deteriorate compared to the throughput of the AMC.

We see in Example 2 that being aggressive is helpful to HARQ (and to HARQ with packet dropping) in the low range of the throughput where we can use higher transmission rates than those suggested by the AMC rate-adaptation $R(\text{snr})$. This provides another way of looking at the problem: the throughput cannot be improved for high throughput values because there are no sufficiently high rates in the set \mathcal{R} ; here $\max\{\mathcal{R}\} = 4$ since a 16-QAM modulation is used. However, extending the range of operation, that is, adding new rates to \mathcal{R} will merely offset the problem: in any system, there is always a maximum transmission rate, and HARQ will always fail to improve the throughput in the range that is close to $\max\{\mathcal{R}\}$.

E. Upper Layers: Why We Ignore The Packet Loss at the PHY

Fig. 1 shows two layers that are responsible for the retransmission: LLC, which implements the ARQ protocol, and PHY, which implements AMC (and possibly also HARQ). Since the PHY cannot guarantee a successful transmission, the packet contents is kept in the LLC buffer till a successful decoding is declared. In this way, some bits may require many PHY transmissions before being successfully decoded at the receiver. The introduction of ARQ at LLC guarantees a zero-outage and yet does not affect the throughput seen by the upper layers [27, Sec. II.A]. Such a double-retransmission mechanism is adopted in LTE [29, Ch. 12], where ARQ is activated when dealing with loss-sensitive but delay-tolerant applications.

⁹In practice, the exhaustive search is not feasible and the optimization is implemented via the on-line adaptation: Δ is fine-tuned using slow-feedback trying to maximize a parameter of interest—here the throughput. While Δ can take any positive value, the space of possible values Δ considered in the numerical example is logarithmically spaced between 1 and Δ_{max} , where Δ_{max} guarantees that R_L is always available for adaptation, i.e., $\Delta_{\text{max}} \cdot \text{snr} \geq \gamma_{[L]}$ for all values of snr we consider.

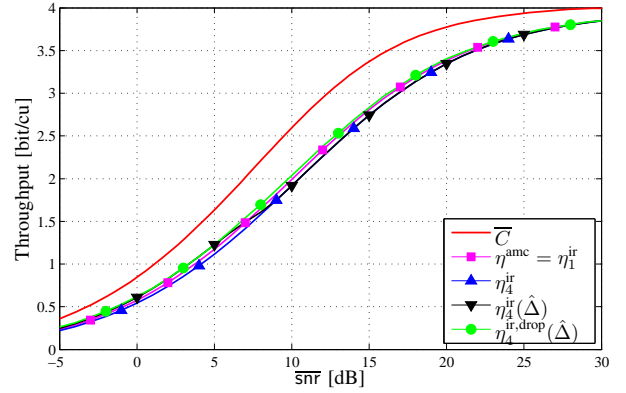


Fig. 2. 16-QAM over Rayleigh fading channels with $f_D\tau = 0.05$; the throughput of the conventional IR-HARQ with the AMC rate adaptation, η_K^{ir} as well as with the aggressive rate adaptation $\eta_4^{\text{ir}}(\hat{\Delta})$ are compared to the throughput of IR-HARQ with packet dropping $\eta_4^{\text{ir,drop}}(\hat{\Delta})$. The ergodic capacity, \bar{C} (19) is shown for reference.

Another scenario where the outage can be ignored is when the Fountain coding [38] is used at the application layer: the T application packets $\mathbf{b}[t], t = 1, \dots, T$ are transformed/encoded into a potentially unlimited number of information packets $\mathbf{m}[1], \mathbf{m}[2], \dots$. This is done in such a way that we can recover/decode all packets $\mathbf{b}[t]$ from *any* subset of $T + \tau$ packets $\mathbf{m}[n]$, where $\tau \ll T$. Thus, at the receiving end, we do not care if the decoding of *each* of the packets $\mathbf{m}[n]$ succeeds but only require having $T + \tau$ of them decoded correctly. In other words, the throughput is what really counts and we can ignore the actual value of the packet loss probability.

III. AMC AND LAYER-CODED HARQ

In Example 2, we explained how the retransmissions in HARQ could penalize the throughput. We also identified the source of the problem: in the conventional HARQ, the adaptation to the channel occurs only in the first transmission round when the AMC-like behavior is used to exploit the CSI snr_1 ; all subsequent rounds *ignore* the CSIs $\text{snr}_2, \dots, \text{snr}_K$.

On the other hand, the AMC alone discards the past channel observations \mathbf{y} independently whether the decoding was successful or not. This clearly is a waste of resources and we want to combine now the adaptability of AMC and the capacity of HARQ to exploit the past observations.

A. Variable-length HARQ vs L-HARQ

The problem of throughput penalty occurring when HARQ is combined with the AMC was partially remedied by the packet dropping, see Sec. II-D, where the CSI is used to decide whether to retransmit the undecoded packet using the entire channel block or to drop it definitely. A variable-length HARQ (VL-HARQ), studied in e.g., [7], [13], [22]–[26], may be seen as a compromise between the very crude adaptation of packet dropping and non-adaptive, conventional HARQ. The idea is to encode an information packet \mathbf{m} into a sequence of subcodewords $\mathbf{x}_1, \dots, \mathbf{x}_K$, whose length, i.e., the number of symbols they are composed of, $N_{s,k}$, may vary from one subcodeword to another. We assume that the number of symbols

in the first codeword is fixed $N_s = N_{s,1}$, i.e., $\mathbf{x}_1 \in \mathbb{R}^{R_1 N_s}$, and for convenience, we normalize the length of the remaining ones via $\ell_k \triangleq N_{s,k}/N_s$.

The optimization problem we have to solve is to find the values $R_1, \ell_2, \dots, \ell_K$ which maximize the throughput of VL-HARQ. However, we cannot simply adopt the solutions developed previously in [25], [26] because they did not deal with the instantaneous CSI; others, e.g., [7], [13], targeted particular values of the PER, which is not of concern in our paper. More importantly, in this work we admittedly ignore the knowledge of the distribution of the SNR; see comments after (16).

Therefore, for comparison purpose we will propose a new approach which is detailed in Example 4. What is important to understand at this point is that any adaptation will be based on the PER function which is defined for each HARQ round

$$\begin{aligned} \text{PER}_k(\text{snr}_k, \ell_k; \cdot) \\ \triangleq \text{PER}(\text{snr}_k, \ell_k; \{\tilde{\text{snr}}_t\}_{t=2}^{k-1}, R_1, \{\ell_t\}_{t=2}^{k-1}) \end{aligned} \quad (24)$$

and which depends on the following arguments:

- the SNR estimated before the k th transmission round, snr_k ;
- the length, ℓ_k of the subcodeword \mathbf{x}_k used in the k th round;
- all past channel SNRs, $\tilde{\text{snr}}_1, \dots, \tilde{\text{snr}}_{k-1}$; and
- all transmission parameters chosen in the previous rounds, i.e., $R_1(\text{snr}_1)$, and $\ell_t(\text{snr}_t), t = 2, \dots, k-1$.

It is immediately clear that, in the case of the practical encoders/decoders, finding empirically the PER function (24) with so many parameters presents a considerable challenge. This is the main reason why the previous works on the variable-length HARQ used simplifying assumptions to take care of its large number of arguments. For example, [26] assumed that the receiver's PER function is binary and the error events are defined in a way similar to (22); [1], [13] used analytical PER functions which have to be fit to the actual decoding curves. Similarly, while the empirical decoding curves are used in [24], [25] the approximations are still necessary to predict the performance for arbitrary values of the SNR and the codeword length.

Besides the practical difficulty of describing the PER function, there is also another important, system-level consideration: VL-HARQ uses only fraction of channel resources which goes against the goal of assigning fixed resources to each of the HARQ rounds. Additional assumptions are then required. In particular, [4], [13] let the user to transmit variable number of packets within a fixed-length *frame*. This, however, raises a problem of resource assignment to many packets in the frame as well as implies the signalling overhead: the length of the codeword of each packet in the frame must be indicated.

L-HARQ, addresses the above difficulties as follows: instead of transmitting the new (redundant) coded symbols $\mathbf{x}_k, k = 2, \dots, K$ to enable the decoding of the packet \mathbf{m}_1 , transmitted in the first round, we rather transmit (some of) the bits of the packet \mathbf{m}_1 (we denote these redundant bits as \mathbf{m}'_1), and we “fill” the remaining space with a fresh content \mathbf{m}_2 . So the conventional channel coding is preceded by the mixing of

the punctured information packets; this is the idea of layered-coding, L-HARQ, proposed in [2] and modified in [3]. The decoding is also done in layers, where the mixed packets \mathbf{m}'_1 and \mathbf{m}_2 are decoded first and, next, the packet \mathbf{m}_1 is recovered with the aid of \mathbf{m}'_1 .

The main advantages are that *i*) the channel coding is not affected by the packet mixing and can be implemented without joint-coding considerations, *ii*) the decoding is straightforward and can be done with commercially available decoders as demonstrated in [3], and finally *iii*) the decoding results are described by one-dimensional PER curves which depend only on one SNR; the dependence of the decoding results on other SNRs is implicit and defined via recursive (layered) decoding.

Using fixed resources at the PHY may be seen as a way to reduce the signaling overhead and to ease the resource management (required, e.g., for the scheduling in multi-user systems [29, Ch. 12.1]). A cautionary note is in order here: the choice of a particular transmission strategy is a complex issue which depends on many system-level elements that are difficult to include in the PHY-level analysis/design.

B. L-HARQ Example: $K = 2$

To explain the details, it is easier to start with the simplest case of HARQ, i.e., when $K = 2$.

Transmitter

The first transmission is done as in the conventional AMC: using the rate R_1 , the packet $\mathbf{m}_1 \in \{0, 1\}^{R_1 \cdot N_s}$ is encoded and the resulting codeword, $\mathbf{x}_1 = \Phi[\mathbf{m}_1]$ is transmitted over the channel. Then, if the decoding succeeds, $\hat{\mathbf{m}}_1 = \mathbf{m}_1$ (an ACK is fed back), the earned reward is given by $R[n] = R_1$ and we move to the next packet. If the decoding fails, $R[n] = 0$. The average reward attainable in the first round is thus the same as in the case of the AMC: $R[n] = R_1(1 - \text{PER}(\text{snr}_1; R_1))$.

When the decoding fails, i.e., ERR_1 is observed, in the next channel block, we implement the second round of HARQ. First, we choose the channel coding rate R_2 . This is similar to the conventional AMC. However, we now encode the packet $\mathbf{m}_{[2]}$ which is a mix of two subpackets: $\mathbf{m}'_{[1]}$, which contains “old” bits taken from the unsuccessfully transmitted packet \mathbf{m}_1 ,¹⁰ and the subpacket \mathbf{m}_2 , composed of “new” bits

$$\mathbf{m}_{[2]} = [\mathbf{m}'_{[1]}, \mathbf{m}_2] \in \mathbb{B}^{R_2 N_s} \quad (25)$$

$$\mathbf{m}'_{[1]} = \Phi_1^b[\mathbf{m}_1] \in \mathbb{B}^{\rho_1 N_s}, \quad (26)$$

where ρ_1 is the packet-mixing rate, i.e., $\mathbf{m}'_{[1]}$ contains $\rho_1 N_s$ bits of \mathbf{m}_1 , and therefore, the natural constraint here is $\rho_1 < \min\{R_1, R_2\}$: the packet $\mathbf{m}'_{[1]}$ cannot contain more bits than $\mathbf{m}_{[2]}$ or \mathbf{m}_1 .

The channel coding is done as before, i.e., $\mathbf{x}_2 = \Phi[\mathbf{m}_{[2]}]$.

Receiver

At the receiver, initially, we ignore the particular structure of the packet $\mathbf{m}_{[2]}$, and we decode it as $\hat{\mathbf{m}}_{[2]} = \text{DEC}[\mathbf{y}_2]$. Again, we obtain the reward $R[n] = R_2$ or $R[n] = 0$; this is how the conventional AMC would work. However, if we decode the packet $\mathbf{m}_{[2]}$, we may exploit the structure (25). In particular,

¹⁰In other words, $\mathbf{m}'_{[1]}$ is a punctured version of \mathbf{m}_1 .

$m'_{[1]}$ provides a priori information about m_1 and can be used in the “backtrack” decoding

$$\hat{m}'_{[1]} = \text{DEC}[\mathbf{y}_1; m'_{[1]}] \quad (27)$$

as proposed in [2]. We define the backtrack decoding error as $\text{ERR}_1^b \triangleq \{\hat{m}'_{[1]} \neq m_{[1]}\}$ and describe its probability by the backtrack PER function

$$\begin{aligned} \text{PER}^b(\tilde{s}\tilde{n}r; R, \rho) &\triangleq \Pr \left\{ \text{ERR}^b | \text{ERR}, \tilde{\text{SNR}} = \tilde{s}\tilde{n}r, R, \rho \right\} \quad (28) \\ &= \frac{\Pr \left\{ \text{ERR} \wedge \text{ERR}^b | \tilde{\text{SNR}} = \tilde{s}\tilde{n}r, R, \rho \right\}}{\Pr \left\{ \text{ERR} | \tilde{\text{SNR}} = \tilde{s}\tilde{n}r, R \right\}}, \end{aligned} \quad (29)$$

which depends on the SNR, $\tilde{s}\tilde{n}r$, that was actually observed in the first round.

The PER function (28) must decrease with ρ : from the information-theoretic point of view, the decoding (27) can succeed, even if the decoding $\text{DEC}[\mathbf{y}_1]$ has failed, because the uncertainty about the packet m_1 (i.e., the rate at which the unknown bits are coded) is decreased. From the practitioner’s point of view, knowing $m'_{[1]}$, we have absolutely certain a priori information about the information/systematic bits $m'_{[1]}$ from the packet m_1 , which improves the performance of the decoder.¹¹

Since we may now recover the entire packet m_1 (having $m'_{[1]}$ means that m_1 was partially decoded in the second round), the reward for the second cycle is calculated as

$$R[n] = \left[R_2 + (R_1 - \rho_1)(1 - \text{PER}^b(\tilde{s}\tilde{n}r_1; R_1, \rho_1)) \right] (1 - \text{PER}(\text{snr}_2; R_2)), \quad (30)$$

here, since $m'_{[1]}$ is common in both transmission rounds, the associated reward, ρ_1 , is already included in R_2 ; thus, we subtract ρ_1 from R_1 to avoid counting this reward twice.

The only remaining question is how to choose the rates R_1 , R_2 , and ρ_1 , but we postpone the discussion until we formulate the solution for an arbitrary number of rounds.

C. L-HARQ: General Case

We now generalize the encoding/decoding to $K > 2$; we explain and separate the encoding/decoding and adaptation operations in the flowchart shown in Fig. 3.

Transmitter

In each round, the encoding is done in two steps. First, we do a binary packet mixing: the old packet $m_{[k-1]}$ is punctured, using rate ρ_{k-1} , yielding a subpacket $m'_{[k-1]} = \Phi_{k-1}^b[m_{[k-1]}]$ according to Eq. (i) in Fig. 3;¹² the resulting $m'_{[k-1]}$ is concatenated with new information bits m_k to form the packet $m_{[k]} = [m'_{[k-1]}, m_k]$, see Eq. (ii). Second, the channel encoding: Eq. (iii) straightforwardly encodes $m_{[k]}$ using the rate R_k .

Receiver

¹¹For example, in iterative binary decoders, knowing some of systematic bits corresponds to setting the corresponding logarithmic likelihood ratios (LLRs) to $\pm\infty$.

¹²The equations on Fig. 3 are labeled with a roman numerology and this is the reason we explicitly use the abbreviation “Eq.”.

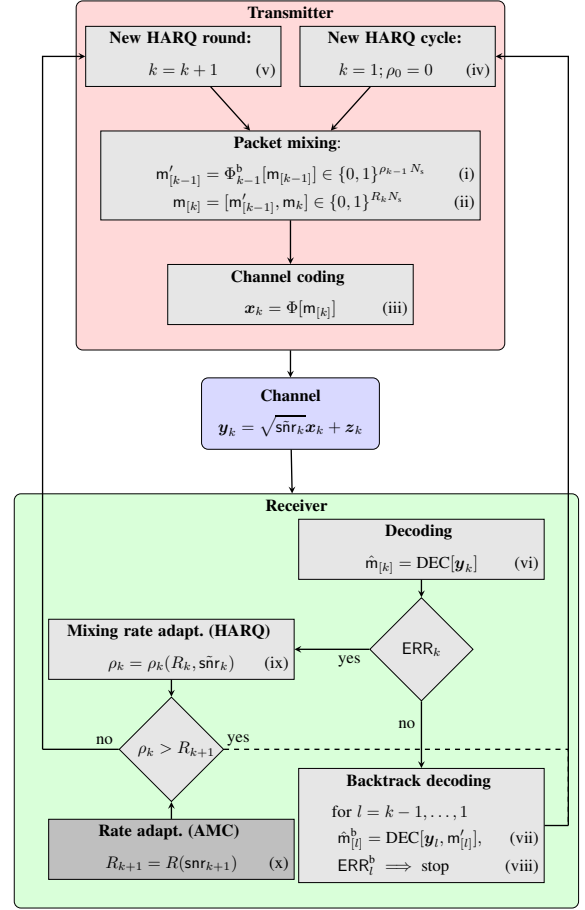


Fig. 3. Actions flow at the transmitter and the receiver in the proposed L-HARQ. The rate adaptation at the receiver is composed of the two parts: the mixing rate adaptation (ix) proper to HARQ which follows the decoding error ERR_k , and the channel rate adaptation Eq. (x) proper to the AMC. The adaptation results are used by the transmitter independently in two encoding steps Eq. (i) and Eq. (ii). Their dependence shows up only if $\rho_k > R_{k+1}$, which may terminate the HARQ cycle, as shown by the dashed transition line at the receiver.

Using only the observation \mathbf{y}_k , the receiver starts the first step of the decoding process Eq. (vi).

- If the packet $m_{[k]}$ is decoded correctly in the k -th round, i.e., $\hat{m}_{[k]} = m_{[k]}$, we recover the message $m'_{[k-1]}$ and m_k according to Eq. (ii). With $m'_{[k-1]}$ and \mathbf{y}_{k-1} known in the k -th round, we “backtrack” decode the packet $m_{[k-1]}$ according to Eq. (vii). If the backtrack decoding $m_{[k-1]}$ is successful, i.e., $\hat{m}_{[k-1]}^b = m_{[k-1]}$, we then recover m_{k-1} and $m'_{[k-2]}$ according to Eq. (ii). In this way, we continue the backtrack decoding to recover all the packets m_{k-2}, \dots, m_1 . However, if a backtrack decoding error, $\text{ERR}_l^b = \{\hat{m}_{[l]}^b \neq m_{[l]}\}$, is observed for any packet $l \in \{k-1, \dots, 1\}$, we abandon the decoding and declare the packets from the previous rounds, m_l, m_{l-1}, \dots, m_1 lost.
- If an error

$$\text{ERR}_k = \{\hat{m}_{[k]} \neq m_{[k]}\} \quad (31)$$

is observed, we have to prepare the packet $m_{[k+1]}$ for the next HARQ round. To this purpose and according

to Eq. (i) and Eq. (ii), we need to determine the mixing ρ_k and the transmission rate R_{k+1} , respectively. In particular, we consider that ρ_k is a function of R_k and $\tilde{\text{snr}}_k$, i.e., $\rho_k \equiv \rho_k(R_k, \tilde{\text{snr}}_k)$ and the way to obtain the adaptation function $\rho_k(R_k, \tilde{\text{snr}}_k)$ will be explained in Sec. III-E. On the other hand, the transmission rate R_{k+1} is available only after the receiver observes/estimates snr_{k+1} , see Eq. (x). Finally, we compare ρ_k to the rate of the next transmission R_{k+1} in order to decide whether the new HARQ round can be done, see Eq. (v), or the HARQ cycle should be restarted, see Eq. (iv).

We emphasize here that the two-steps decoding adopted in L-HARQ is not the only option: it is possible for instance, to perform the joint decoding of all packets m_1, \dots, m_k using all channel outcomes $\mathbf{y}_1, \dots, \mathbf{y}_k$ as proposed in [21].¹³ However, motivated by the fact that the simplified encoding-decoding schemes adopted in L-HARQ do not impose any throughput penalty [30, Th. 3], and to keep the backtrack decoding simple, we do not consider any of those possibilities here.

D. Optimal Rate Adaptation

While the operations of the transmitter and the receiver are simple, we still must adapt the transmission rates R_k and the mixing rates ρ_k . For the purpose of the discussion, it is convenient to write clearly the rewards earned in each round, which generalizes (30). Namely,

$$R_k = (R_k + J_k)(1 - \text{PER}(\text{snr}_k; R_k)) \quad (32)$$

$$J_k = (J_{k-1} + R_{k-1} - \rho_{k-1}) (1 - \text{PER}^b(\tilde{\text{snr}}_{k-1}; R_{k-1}, \rho_{k-1})), \quad (33)$$

where J_k is the reward that can be obtained in the k -th HARQ round thanks to the backtrack decoding.

The above allows us to formulate the problem using a Markov decision process (MDP) formalism, where we define the *states* as a tuple

$$\mathbf{s}_k \triangleq (J_{k-1}, \text{snr}_k, \tilde{\text{snr}}_{k-1}, R_{k-1}), \quad (34)$$

and the objective is to find the optimal *actions* for each state \mathbf{s}_k

$$\mathbf{a}_k \triangleq (R_k, \rho_{k-1}) = \pi(\mathbf{s}_k), \quad (35)$$

where $\pi(\cdot)$ is the adaptation function or – the *policy*. Since knowing the action \mathbf{a}_k determines the transition probability from state \mathbf{s}_k to state \mathbf{s}_{k+1} , and the reward depends solely on the state and the action, the optimal policy which maximizes the reward can be found using known algorithms, such as policy iteration or value iterations [39, Chap. 7].

While, the MDP leads to a very efficient optimization, its implementation may still be challenging if the dimension of the space is large. Here, unfortunately, this is the case: even if we assume that the available transmission rates, R_k , are discrete, the three arguments remaining in (34) are continuous. The problem is thus hardly tractable numerically.

Moreover, we can argue that, while finding the optimal rate adaptation functions is theoretically interesting, its practical

value is much less important because *i*) the optimal solution would depend on the fading distribution, e.g., defined by (7), which we consider impractical since the latter is not known, see comments after (15); and *ii*) the rate adaptation function would be multidimensional (would depend on as many parameters as there are dimensions in the state of the MDP; here, four dimensions), which is not only tedious to implement but also makes the AMC and HARQ adaptations coupled; which goes against the simplicity of the AMC adaptation which we consider a valuable feature.

Therefore, the simplifications and the heuristic solutions we propose may turn out to be not only viable but also more *practical* alternatives to the complex solutions that can be obtained from the optimization defined by the MDP framework. Having said this, we believe it would be interesting to find these optimal solutions; first, to verify how far our heuristic solution falls from the optimality; second, to obtain a better insight into the importance of the observed parameters of the state \mathbf{s}_k and, possibly, to derive other useful heuristics.

E. Simplified Rate Adaptation

We will propose simple, and intuitively justified heuristics, where we target the independence of adaptation strategies between AMC (here, the choice of R_k) and HARQ (here, the choice of the packet mixing rate ρ_{k-1}).

First of all, we decide to adapt the coding rates in the same way irrespectively of the past HARQ transmission rounds

$$R_k(\text{snr}) = R(\text{snr}), \quad (36)$$

where $R(\text{snr})$ is the AMC rate-adaptation policy we found in (15) and which we can also eventually enhance with the fine-tuning (17). This can be seen as a maximization of the instantaneous reward R_k in (32) setting $J_k = 0$.

Second, we have to decide what packet mixing rate ρ_{k-1} should be used in the k -th round. The first simplification due to the AMC approach (36) is that we make ρ_{k-1} independent of snr_k , i.e.,

$$\rho_k = \rho_k(R_k, \tilde{\text{snr}}_k). \quad (37)$$

Next, from (33), we see that small ρ_{k-1} increases the potential reward (given by $R_{k-1} - \rho_{k-1}$ in (33)), yet it has to be sufficiently large to make the backtrack PER , $\text{PER}^b(\tilde{\text{snr}}_{k-1}; R_{k-1}, \rho_{k-1})$, low. The latter requirement is also needed to recover all the packets from the previous rounds because we decided to abandon all of them once we observe the backtrack decoding error, ERR^b , see Eq. (viii).

To strike a balance between these two requirements, we decide to choose the minimum packet-mixing rate to attain the prescribed value of the backtrack PER , ϵ_b

$$\rho_{k-1} = \begin{cases} 0 & \text{if } \text{PER}^b(\tilde{\text{snr}}_{k-1}; R_{k-1}, R_k) > \epsilon_b \\ \min_{\rho < R_k} \{\rho \in \mathcal{R}_b : \text{PER}^b(\tilde{\text{snr}}_{k-1}; R_{k-1}, \rho) \leq \epsilon_b\} & \text{o.w.} \end{cases} \quad (38)$$

where the first condition line in (38) takes care of the case when it is impossible to attain the PER value of ϵ_b ;¹⁴ then, we

¹⁴The PER function $\text{PER}^b(\tilde{\text{snr}}_{k-1}; R_{k-1}, \rho)$ is decreasing with ρ , and attains its minimum for the maximum admissible value of $\rho = R_k$.

¹³Another decoding scheme was also proposed in [3, footnote 2].

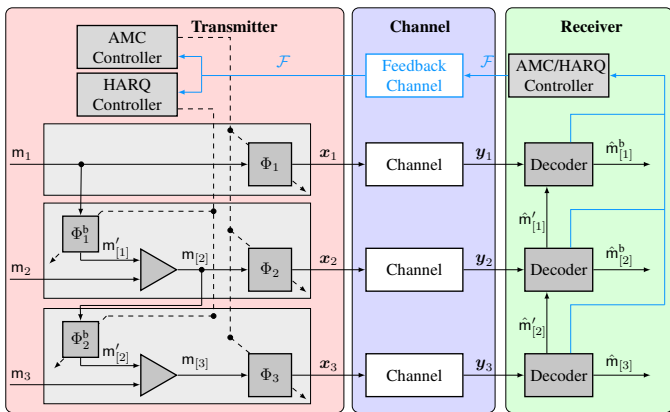


Fig. 4. Encoding and decoding in L-HARQ. The AMC controller adjusts the rate of the channel encoder, Φ_k , independently of the HARQ which selects the packet-mixing rate (i.e., the rate of the puncturer $\Phi_k^b[\cdot]$). The decoding is done block-by-block using the channel outcome \mathbf{y}_k and $\hat{\mathbf{m}}'_k$, i.e., $\hat{\mathbf{m}}^b_k = \text{DEC}[\mathbf{y}_k; \hat{\mathbf{m}}'_k]$. We assume here that $K = 3$ rounds are carried out, where ERR_1 and ERR_2 are observed (the first and the second rounds are in error) and the third HARQ round is successful, i.e., $\hat{\mathbf{m}}_{[3]} = \text{DEC}[\mathbf{y}_3] = \mathbf{m}_{[3]}$; the backtrack decoding is then successful as well, which means that $\hat{\mathbf{m}}^b_k = \text{DEC}[\mathbf{y}_k; \hat{\mathbf{m}}'_k] = \mathbf{m}_{[k]}$, $k \in \{2, 1\}$.

set $\rho_1 = 0$, which means that $\mathbf{m}_{[k]} = \mathbf{m}_k$, see Eq. (i)–Eq. (ii), and this is equivalent to dropping the packet $\mathbf{m}_{[k-1]}$ and starting a new HARQ cycle; \mathcal{R}_b denotes the set of available mixing rates.

Since, *after* the k -th round, the receiver knows both the value of snr_k and $R_k = R(\text{snr}_k)$, it can calculate also ρ_k via (38), and, before the round $k + 1$ starts, ρ_k can be sent to the transmitter together with R_{k+1} using the feedback \mathcal{F} .

The structure of the transmitter and the receiver is shown in Fig. 4. The important element is that the coding and the adaptation to the CSI/SNR is done by the AMC independently of the operation of HARQ. We also note that we still maintain a certain degree of adaptability with a fine-tuning (17) for the rate-adaptation in the AMC controller, and with the possible adjustment of the target backtrack PER, ϵ_b .

IV. EXAMPLES

We note first that the operation of the L-HARQ is solely based on the conventional AMC and the added step of packet mixing. We emphasize again that the formulas presented up to now do not take into account any prior knowledge about the statistical behavior of the channel. That is, while we will use Rayleigh fading (7) to model the SNRs, we do not exploit this knowledge in the design of HARQ.¹⁵

Example 3 (16-QAM & 64-QAM, Rayleigh fading, threshold decoding, continuation of Example 2). *Using the threshold decoding approach from Example 2, the decoding errors are deterministically defined by the MI in (22) and interpreting the*

¹⁵Although the joint distribution (8) is used in (4) to define the PER function, this is done for the sake of numerical comparison. In practice we will rather use the thresholds $\gamma_{[L]}$ estimated by the transmitter as in (6); this can be done via slow-feedback adaptation measuring the value of the PER without knowing the entire PER function.

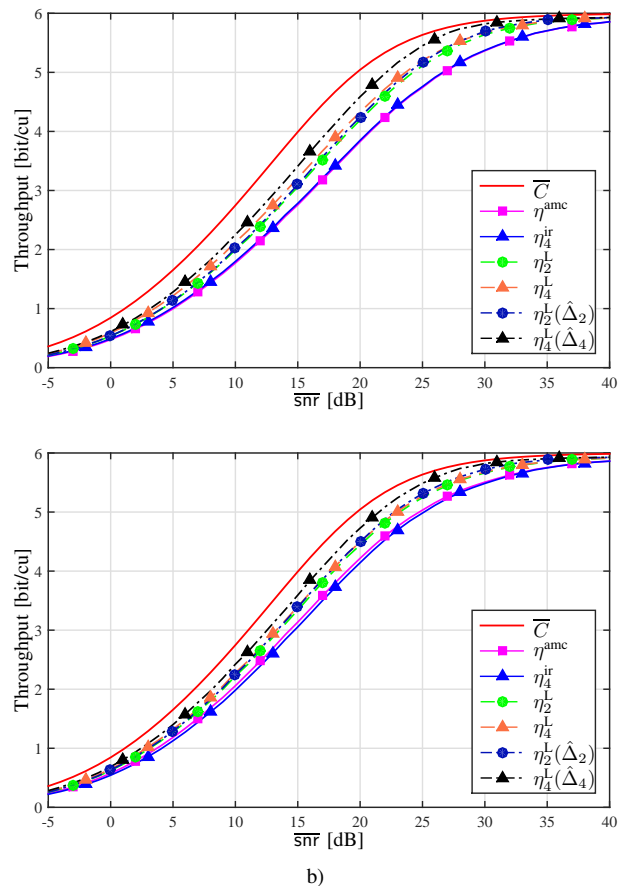


Fig. 5. 16-QAM & 64-QAM transmission over Rayleigh fading channels; threshold decoding model. Throughput of the proposed L-HARQ, $\eta_K^L(\Delta)$, is compared to the conventional IR-HARQ, η_K^r , when a) $f_D\tau = 0.1$, i.e., $\delta \approx 0.8$, and b) $f_D\tau = 0.05$, i.e., $\delta \approx 0.95$.

knowledge of $\mathbf{m}'_{[1]}$ as decrease of the information rate from R_1 to $R_1 - \rho_1$, the error event is defined as

$$\text{ERR}_k^b = \{I(\text{snr}_k) < R_k - \rho_k\}. \quad (39)$$

Consequently, we can transform (38) into

$$\rho_k = R_k - I(\text{snr}_k), \quad (40)$$

which holds for any $\epsilon_b \geq 0$ if we assume that the set of backtrack rates, denoted \mathcal{R}_b , is continuous, i.e., $\mathcal{R}_b \in [0, R_k]$. This idealized assumption will be relaxed in Example 5.

With the AMC-optimal rate-adaptation policy $R(\text{snr})$, having the rate-mixing function (40), as well as the decoding error events defined by (22) and (39), we can run the Monte-Carlo simulation. The throughput of the proposed L-HARQ, η_K^L is shown in Fig. 5, where we compare it with IR-HARQ for two different values of the normalized Doppler frequency, $f_D\tau \in \{0.1, 0.05\}$. We assume that both 16 and 64-QAM constellations are used, i.e., the set of available rates is defined as $\mathcal{R} = \{R_c M \mid M \in \{4, 6\}, R_c \in (0, 1]\}$. Here, R_c may be understood as the rate of a binary encoder whose output is interleaved and then used by the modulator; thus we assume a bit-interleaved coded modulation (BICM) is implemented [37].

We can see clearly that allowing modulation order adaptation does not change the conclusions drawn in Example 2,

i.e., adding the conventional IR-HARQ on top of AMC does not provide gains from throughput of view. However, the gains provided by L-HARQ over the conventional IR-HARQ are notable already for $K = 2$. For instance, for a target throughput value of $\eta \in (2.5, 5)$ bit/cu, the SNR gap between the conventional IR-HARQ and the ergodic capacity is reduced by approximately 2dB. On the other hand, increasing the number of transmissions to $K = 4$ does not increase the gains. This is because the rate-adaptation policy of AMC is set irrespectively of the fact that HARQ takes care of undecoded packets; it is thus defined conservatively to avoid “too many” decoding errors.

To take advantage of HARQ, and improve the throughput, AMC must use a more aggressive rate adaptation; this can be done via fine-tuning defined in (17). The throughput of such aggressive L-HARQ, $\eta_K^L(\hat{\Delta})$ is also shown in Fig. 5, where we see that by allowing for more rounds, e.g., $K = 4$, L-HARQ yields results even closer to the ergodic capacity, gaining another 1–2dB. This is achieved by using rates that are higher than those indicated by AMC as shown in Fig. 6; we can see clearly that the optimal $\hat{\Delta}$ tends to increase when K increases. The transmission rate becomes more aggressive with larger K because more errors can be tolerated initially and the decoding is postponed to the later rounds.

We observed that the optimal value $\hat{\Delta}$ increases slowly in low-to-medium $\overline{\text{snr}}$ but tends to increase faster for high SNR. For instance, in the case of $K = 4$ and $f_D\tau = 0.05$, we obtained $\hat{\Delta} \in (1.2, 3.4)$ for $\overline{\text{snr}} \in (-5, 20)$ dB while for $\overline{\text{snr}} = 36$ dB, we had $\hat{\Delta} \approx 50$. However, using $\Delta \approx 4$ even for high SNR does not cause a notable throughput penalty compared to $\hat{\Delta}$.

Example 4 (L-HARQ and previous works). The threshold decoding assumption used in the Example 3 provides us with the framework suitable for comparison with previous works which were also based on the similar assumption. Since, using various constellations does not alter the main conclusions we consider only 16-QAM modulation i.e., $\mathcal{R} = \{4R_c \mid R_c \in (0, 1]\}$.

We start by comparing L-HARQ and VL-HARQ introduced in Sec. III-A. As we said in Sec. III-A we have to devise a strategy to adapt the lengths $\ell_k, k = 2, \dots, K$ in each HARQ round. Because we want the adaptation to be independent of the distribution of the CSI, we continue in the spirit of equation (15). Namely, we propose to determine R_1 as in AMC, i.e., exactly following (15), and find ℓ_2, \dots, ℓ_K by maximizing the per-round (instantaneous) throughput, which boils down to solving the following one-dimensional optimization problem:

$$\ell_k(\text{snr}_k) = \underset{\ell \in (0,1)}{\text{argmax}} \frac{R_1(\text{snr}_1)}{\ell} \left(1 - \text{PER}_k(\text{snr}_k, \ell; \cdot)\right), \quad (41)$$

where $\text{PER}_k(\text{snr}_k, \ell; \cdot)$ is defined by (24) and, using the

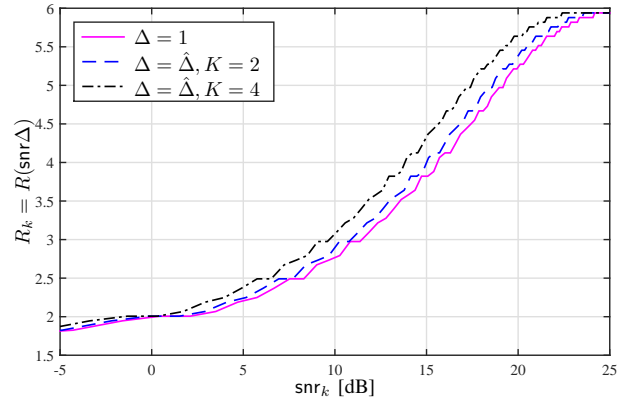


Fig. 6. Example of the optimal rate policy of L-HARQ when $f_D\tau = 0.05$ and $\overline{\text{snr}} = 20$ dB. $\Delta = 0$ means that the AMC policy (16) is used; $\Delta = \hat{\Delta}$ means aggressive adaptation (17) with an optimized aggressiveness factor.

threshold decoding model, it is given by

$$\begin{aligned} & \text{PER}\left(\text{snr}_k, \ell; \{\tilde{\text{snr}}_t\}_{t=1}^{k-1}, R_1, \{\ell_t\}_{t=2}^{k-1}\right) \\ &= \Pr \left\{ \sum_{l=1}^{k-1} \ell_l(\text{snr}_l) I(\tilde{\text{snr}}_l) + \ell I(\tilde{\text{SNR}}_k) < R_1(\text{snr}_1) \right. \\ & \quad \left. \mid \text{SNR}_k = \text{snr}_k \right\} \end{aligned} \quad (42)$$

and can be found using Monte-Carlo simulations for any given R_1 and snr_k . Despite the simplifying threshold decoding assumption, this is still a tedious exercise.

For completeness, we show also the results where the CSI is not available at the transmitter which should highlight the value of combining HARQ and AMC. We use here the cross-packet HARQ (XP-HARQ) derived in [21, eq. (37)].

The results are shown in Fig. 7, where we can see that L-HARQ and VL-HARQ are practically the same for $K = 4$. It is also clear that the XP-HARQ without CSI is equivalent to the conventional IR-HARQ at low-medium $\overline{\text{snr}}$. However, since in very high SNR regime the highest available rate is practically always used, XP-HARQ results (without CSI) are the same as those of L-HARQ (with CSI).

We emphasize that, while we made the operation conditions as similar as possible, the results of VL-HARQ and XP-HARQ should be seen as a “ballpark” figure rather than the rigorous comparison. As for VL-HARQ, this is because we do not consider any constraints on the lengths, i.e., we ignore the issue of sharing the constant-length frame between many packets (of different lengths). As for XP-HARQ, the comparison is not fair neither because, in the absence of the instantaneous CSI, we adapt the length using the distribution of the CSI.

The results in the previous example indicate that L-HARQ presents a notable gain compared to conventional IR-HARQ assuming that *i*) the sets of transmission, \mathcal{R} , and backtrack, \mathcal{R}_b , rates are continuous, *ii*) the error event ERR_k is fully described by the accumulated MI, cf. (39), which also allows us to determine the optimal backtrack rates ρ_k in closed-form, see (40). The purpose of the next example is to compare L-HARQ with IR-HARQ when these idealized assumptions are

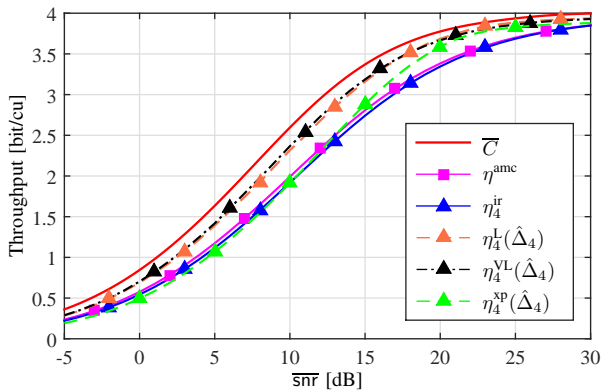


Fig. 7. 16-QAM transmission over Rayleigh fading channels; threshold decoding model. Throughput of the proposed L-HARQ, $\eta_K^L(\Delta)$, is compared to VL-HARQ, $\eta_K^{VL}(\Delta)$, to XP-HARQ, $\eta_K^{XP}(\Delta)$, and to the conventional IR-HARQ, η_K^{IR} ; $f_D\tau = 0.05$, i.e., $\delta \approx 0.95$.

abandoned and practical encoders/decoders are used.

We immediately say that we cannot follow the idea of comparing L-HARQ with VL-HARQ or XP-HARQ. While we could do it in Example 4, this was done only thanks to the assumption of the idealized threshold decoding. The similar comparison is simply out of reach with current computational resources and time-constraints when we use the practical encoders and decoders.

Example 5 (Practical implementation using turbo codes). We consider encoding of information packets using the $\frac{1}{3}$ -rate 3rd generation partnership project (3GPP) turbo-code followed by a 3GPP rate matching which allows us to obtain rates from $\mathcal{R} = \{1.5, 2.25, 3, 3.75\}$. The encoded bits are then mapped to symbols using a Gray mapping [37, Sec. 2.5.2]. The block size is $N_s = 1024$. In this example again, we use only 16-QAM for \mathcal{X} constellation (i.e., AMC is used with fixed modulation, see footnote 8). At the receiver the LLRs are calculated [37, Sec. 3.3] and fed to the 6-iterations binary decoder based on the Bahl–Cocke–Jelinek–Raviv (BCJR) algorithm implemented in the log domain using the library [40]. The example of the PER curves obtained via simulations are shown in Fig. 8.

After each NACK message, $m'_{[k]}$ is a punctured version of m_k , i.e., $m'_{[k]} = \Phi_k^b[m_k]$ which means that $\rho_k \leq R_k$ by construction. For each available transmission rate R , we use uniformly distributed backtrack rates. Namely, we consider $\mathcal{R}_b(R) = \{kR/F, k \in \{0, 1, \dots, F\}\}$ where $\log_2(F)$ is the number of the additional feedback bits needed to send the index of the chosen ρ_k to the transmitter. In the numerical example, we choose $\log_2(F) = 4$.

Fig. 9 shows $\Pr\{\text{ERR}_k \wedge \text{ERR}_k^b | \tilde{\text{SNR}}_k = \tilde{\text{snr}}_k, R_k, \rho_k\}$ as a function of the SNR experienced in the k -th round, $\tilde{\text{snr}}_k$ for different values of ρ_k when $R_k = 3$. We recall that the event $\{\text{ERR}_k \wedge \text{ERR}_k^b\}$ means that both the “direct” and the “backtrack” decoding of the packet m_k failed. It is clear that as the number of known bits $m'_{[k]}$ increases, i.e., when ρ_k increases, the probability of a failure in the backtrack decoding decreases. We note that when $\rho_k = 0$ we have $\text{ERR}_k = \text{ERR}_k^b$.

The mixing rate policy is defined via (38) with $\epsilon_b = 0.1$,

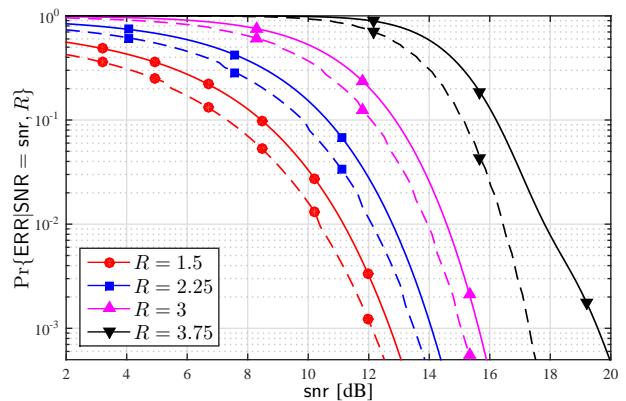


Fig. 8. $\text{PER}(\text{snr}; R) = \Pr\{\text{ERR}[\text{SNR} = \text{snr}, R]\}$ is shown for different values of R and fading defined by (8) with $\delta = 0.95$, i.e., $f_D\tau = 0.05$ and $\overline{\text{snr}} = 15\text{dB}$. The solid lines correspond to a turbo-code transmission with the 16-QAM we use in Example 5, while dashed ones – to the idealized, threshold decoding we use in Example 3.

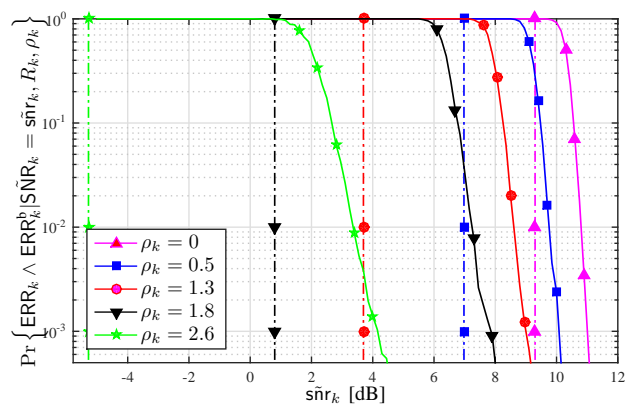


Fig. 9. $\Pr\{\text{ERR}_k \wedge \text{ERR}_k^b | \tilde{\text{SNR}}_k = \tilde{\text{snr}}_k, R_k, \rho_k\}$, shown for $R_k = 3$ and different values of ρ_k , allows us to calculate the backtrack PER function (29). The solid lines correspond to a turbo-code transmission with 16-QAM as in Example 5, while dashed ones – to the idealized, threshold decoding we use in Example 3.

which follows [3, Sec. V.B] and the results of L-HARQ are compared to IR-HARQ in Fig. 10a and Fig. 10b for $f_D\tau = 0.1$ and $f_D\tau = 0.05$, respectively. As already highlighted in Example 2, IR-HARQ is counterproductive in the region of high values of SNR, especially when the estimated snr_k tends to be reliable (large Doppler, $f_D\tau = 0.05$); here, this conclusion is confirmed in the practical setup as well. Furthermore, the gains of L-HARQ with respect to IR-HARQ, theoretically predicted, still materialize in the considered practical scenarios. For instance, when $f_D\tau = 0.1$, the SNR gain of L-HARQ over the conventional IR-HARQ is around 1.5dB for a throughput equal to $\eta = 3\text{bit/cu}$ and $K = 2$. This gain can be increased by using $K = 4$, but the improvement is less important than in the case of the idealized threshold decoding we have shown in Example 3.

This can be understood observing Fig. 9 where we see that for the same value of the SNR $\tilde{\text{snr}}_k$, to make the idealized threshold decoding succeed, the required value of the mixing rate ρ_k is smaller than in the case of the practi-

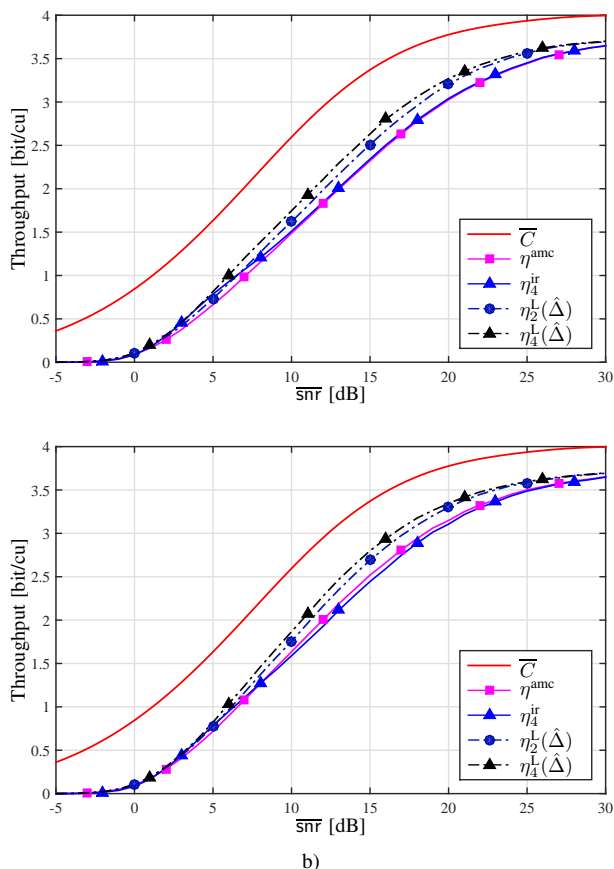


Fig. 10. Turbo-coded 16-QAM transmission over Rayleigh fading channels: throughput of the proposed L-HARQ, $\eta_K^L(\Delta)$, compared to the conventional IR-HARQ, η_K^I , when a) $f_D\tau = 0.1$, i.e., $\delta \approx 0.8$, and b) $f_D\tau = 0.05$, i.e., $\delta \approx 0.95$.

cal codes. This is measured by the SNR-shift of the curve $\Pr\{\text{ERR}_k \wedge \text{ERR}_k^b | \text{SNR}_k = \tilde{\text{snr}}_k, R_k, \rho_k\}$ with respect to the curve $\Pr\{\text{ERR}_k \wedge \text{ERR}_k^b | \text{SNR}_k = \tilde{\text{snr}}_k, R_k, 0\}$; for example, the idealized threshold decoding curve is shifted to the left by $\sim 2.5\text{dB}$ for $\rho_k = 0.5$, while using the turbo-code, this shift is only equal to $\sim 1\text{dB}$. Smaller shift means that higher values of ρ_k must be used to provide the similar guarantees for a successful backtrack decoding, and this translates also into a smaller throughput.

This effect highlights the importance of the suitable coding design which takes into account the reality of the backtrack decoding as it was studied in [3, Sec. IV.B].

We also observed that the aggressivity factor $\hat{\Delta}$ tends to be much smaller in the case of practical decoder/encoder. For instance, $\hat{\Delta} \leq 2$ for all values of SNR when $K = 4$ and $f_D\tau = 0.05$.

V. CONCLUSIONS

This work is motivated by the fact that combining the conventional HARQ with AMC transmissions over i.i.d. block fading channels is detrimental to the throughput when the transmission resources are fixed. As a remedy to this problem, we proposed and analyzed a coding strategy designed to

increase the throughput of HARQ allowing it to exploit the CSI observed at the receiver. The proposed coding strategy is simple to implement because the coding is separated into two logical steps: the channel coding as done in the conventional AMC and the packet mixing done at the bit-level which may be associated with HARQ.

The optimization problem, formulated to find the throughput-maximizing rate adaptation functions, turns out to be infeasibly complex to solve. The heuristic solutions are then proposed and analyzed on examples. Using the information-theoretic approach to coding, and Rayleigh block-fading channels, the throughput obtained thanks to the proposed L-HARQ, shows a gain of 2dB to 4dB when compared to the conventional AMC. In a similar setup, but using the practical, 3GPP turbo-code, the proposed solution shows notable gains of 2dB to 2.5dB. Since these gains are obtained using additional bits in the feedback channel, the tradeoff between the additional signaling and the throughput improvement should be further assessed using system-level considerations.

We conjecture also that the gap between the practical codes and the theoretical limits is due to the particular coding strategy adopted here. The optimization of the coding scheme which would take into account the structure of the decoding scheme, would improve the results as already shown in [3].

Since the proposed adaptation strategy maintains constant resources allocated to each user, we argue that it may be particularly suitable to combine the analysis with the multi-user resource management procedures, a problem which is left for further investigation. Moreover, it would be interesting to compare VL-HARQ and L-HARQ from a system point of view, taking into account additional practical constraints such as feedback costs and channel resource granularity.

REFERENCES

- [1] R. Sassioui, M. Jabi, L. Szczecinski, L. B. Le, M. Benjillali, and B. Pelletier, "HARQ and AMC: Friends or foes?" *IEEE Trans. Commun.*, vol. 65, no. 2, pp. 635–650, Feb. 2017.
- [2] P. Popovski, "Delayed channel state information: Incremental redundancy with backtrack retransmission," in *IEEE Inter. Conf. Comm. (ICC)*, June 2014, pp. 2045–2051.
- [3] M. Jabi, E. Pierre-Doray, L. Szczecinski, and M. Benjillali, "How to boost the throughput of HARQ with off-the-shelf codes," *IEEE Trans. Commun.*, vol. 65, no. 6, pp. 2319–2331, June 2017.
- [4] Q. Liu, S. Zhou, and G. B. Giannakis, "Cross-layer combining of adaptive modulation and coding with truncated ARQ over wireless links," *IEEE Trans. Wireless Commun.*, vol. 3, no. 5, pp. 1746–1755, Sep. 2004.
- [5] H. Zheng and H. Viswanathan, "Optimizing the ARQ performance in downlink packet data systems with scheduling," *IEEE Trans. Wireless Commun.*, vol. 4, no. 2, pp. 495–506, Mar. 2005.
- [6] D. Kim, B. C. Jung, H. Lee, D. K. Sung, and H. Yoon, "Optimal modulation and coding scheme selection in cellular networks with hybrid-ARQ error control," *IEEE Trans. Wireless Commun.*, vol. 7, no. 2, pp. 5195–5201, Dec. 2008.
- [7] J. Ramis and G. Femenias, "Cross-layer design of adaptive multirate wireless networks using truncated HARQ," *IEEE Trans. Veh. Technol.*, vol. 60, no. 3, pp. 944–954, Mar. 2011.
- [8] P. Zhang, Y. Miao, and Y. Zhao, "Cross-layer design of AMC and truncated HARQ using dynamic switching thresholds," in *IEEE Wireless Communications and Networking Conference (WCNC'13)*, 7–10 April, Shanghai, China, Apr. 2013, pp. 906–911.
- [9] C. G. Kang, S. H. Park, and J. W. Kim, "Design of adaptive modulation and coding scheme for truncated hybrid arq," *Wireless Personal Communications*, vol. 53, no. 2, pp. 269–280, Apr. 2010.

- [10] L. Le, E. Hossain, and A. Alfa, "Service differentiation in multirate wireless networks with weighted round-robin scheduling and ARQ-based error control," *IEEE Trans. Commun.*, vol. 54, no. 2, pp. 208–215, Feb. 2006.
- [11] X. Wang, Q. Liu, and G. B. Giannakis, "Analyzing and optimizing adaptive modulation coding jointly with ARQ for QoS-guaranteed traffic," *IEEE Trans. Veh. Technol.*, vol. 56, no. 2, pp. 710–720, Mar. 2007.
- [12] L. Le, E. Hossain, and M. Zorzi, "Queueing analysis for GBN and SR ARQ protocols under dynamic radio link adaptation with non-zero feedback delay," *IEEE Trans. Wireless Commun.*, vol. 54, no. 9, pp. 3418–3428, Feb. 2007.
- [13] G. Femenias, J. Ramis, and L. Carrasco, "Using two-dimensional Markov models and the effective-capacity approach for cross-layer design in AMC/ARQ-based wireless networks," *IEEE Trans. Veh. Technol.*, vol. 58, no. 8, pp. 4193–4203, Oct. 2009.
- [14] M. Poggioni, L. Rugini, and P. Banelli, "QoS analysis of a scheduling policy for heterogeneous users employing AMC jointly with ARQ," *IEEE Trans. Commun.*, vol. 58, no. 9, pp. 2639–2652, September 2010.
- [15] L. Carrasco, G. Femenias, and J. Ramis, "Channel-aware MAC performance of AMC-ARQ-based wireless systems," *EURASIP Journal on Wireless Communications and Networking*, vol. 2013, no. 1, p. 213, Aug 2013.
- [16] J. Harsini, F. Lahouti, M. Levorato, and M. Zorzi, "Analysis of non-cooperative and cooperative type II hybrid ARQ protocols with AMC over correlated fading channels," *IEEE Trans. Wireless Commun.*, vol. 10, no. 3, pp. 877–889, Mar. 2011.
- [17] G. Caire and D. Tuninetti, "The throughput of hybrid-ARQ protocols for the Gaussian collision channel," *IEEE Trans. Inf. Theory*, vol. 47, no. 5, pp. 1971–1988, Jul. 2001.
- [18] R. Sassioui, L. Szczecinski, L. B. Le, and M. Benjillali, "AMC and HARQ: Effective capacity analysis," in *IEEE Wireless Communications and Networking Conference (WCNC'16)*, 3-6 April, Doha, Qatar, 2016.
- [19] P. Larsson, L. K. Rasmussen, and M. Skoglund, "Throughput analysis of ARQ schemes in Gaussian block fading channels," *IEEE Trans. Commun.*, vol. 62, no. 7, pp. 2569–2588, Jul. 2014.
- [20] M. Jabi, A. El Hamss, L. Szczecinski, and P. Piantanida, "Multi-packet hybrid ARQ: Closing gap to the ergodic capacity," *IEEE Trans. Commun.*, vol. 63, no. 12, pp. 5191–5205, Dec. 2015.
- [21] M. Jabi, A. Benyouss, M. L. Treust, E. Pierre-Doray, and L. Szczecinski, "Adaptive cross-packet HARQ," *IEEE Trans. Commun.*, vol. 65, no. 5, pp. 2022–2035, May 2017.
- [22] J.-F. Cheng, Y.-P. Wang, and S. Parkvall, "Adaptive incremental redundancy," in *IEEE Veh. Tech. Conf. (VTC Fall)*, Orlando, Florida, USA, Oct. 2003, pp. 737–741.
- [23] E. Uhlemann, L. K. Rasmussen, A. Grant, and P.-A. Wiberg, "Optimal incremental-redundancy strategy for type-II hybrid ARQ," in *IEEE Intern. Symp. Inf. Theory (ISIT)*, 2003, p. 448.
- [24] E. Visotsky, Y. Sun, V. Tripathi, M. Honig, and R. Peterson, "Reliability-based incremental redundancy with convolutional codes," *IEEE Trans. Commun.*, vol. 53, no. 6, pp. 987–997, Jun. 2005.
- [25] S. Pfletschinger and M. Navarro, "Adaptive HARQ for imperfect channel knowledge," in *2010 International ITG Conference on Source and Channel Coding (SCC)*, Jan. 2010, pp. 1–6.
- [26] L. Szczecinski, S. R. Khosravirad, P. Duhamel, and M. Rahman, "Rate allocation and adaptation for incremental redundancy truncated HARQ," *IEEE Trans. Commun.*, vol. 61, no. 6, pp. 2580–2590, June 2013.
- [27] M. Jabi, M. Benjillali, L. Szczecinski, and F. Labeau, "Energy efficiency of adaptive HARQ," *IEEE Trans. Commun.*, vol. 64, no. 2, pp. 818–831, Feb. 2016.
- [28] S. Verdú and S. Shamai, "Variable-rate channel capacity," *IEEE Trans. Inf. Theory*, vol. 56, no. 6, pp. 2651–2667, Jun. 2010.
- [29] E. Dahlman, S. Parkvall, and J. Skold, *4G LTE/LTE-advanced for mobile broadband*, 2nd ed. Academic Press, 2014.
- [30] K. F. Trillingsgaard and P. Popovski, "Generalized HARQ protocols with delayed channel state information and average latency constraints," *IEEE Trans. Inf. Theory*, vol. PP, no. 99, pp. 1–1, 2017.
- [31] 3GPP, "3GPP TS 36.213 V13.1.1 release 13 (2016-03): LTE; Evolved Universal Terrestrial Radio Access (E-UTRA); Physical layer procedures.".
- [32] M.-S. Alouini and A. J. Goldsmith, "Adaptive modulation over Nakagami fading channels," *Kluwer Journal on Wireless Communications*, vol. 13, no. 1-2, pp. 119–143, May 2000.
- [33] M. Levorato, L. Badia, and M. Zorzi, "On the channel statistics in hybrid ARQ systems for correlated channels," in *IEEE Information Theory Workshop (ITW)*, Oct. 2009, pp. 90–94.
- [34] Y. Hu and A. Ribeiro, "Optimal wireless communications with imperfect channel state information," *IEEE Trans. Signal Process.*, vol. 61, no. 11, pp. 2751–2766, Jun. 2013.
- [35] J. G. Proakis and M. Salehi, *Digital Communications*, 5th ed. McGraw-Hill, 2008.
- [36] P. Wu and N. Jindal, "Performance of hybrid-ARQ in block-fading channels: A fixed outage probability analysis," *IEEE Trans. Commun.*, vol. 58, no. 4, pp. 1129–1141, Apr. 2010.
- [37] L. Szczecinski and A. Alvarado, *Bit-Interlaved Coded Modulation : Fundamentals, Analysis and Design*. Wiley, 2015.
- [38] J. D. Ellis and M. B. Pursley, "Integration of adaptive modulation and channel coding with fountain coding for packet radio systems," *IEEE Trans. Commun.*, vol. 63, no. 5, pp. 1510–1521, May 2015.
- [39] D. P. Bertsekas, *Dynamic Programming and Optimal Control*, 3rd ed. Athena Scientific, 2005, vol. 2.
- [40] E. Pierre-Doray and L. Szczecinski. (2015) "FeCl channel coding library". [Online]. Available: <https://github.com/eti-p-doray/FeCl/wiki>